



## CHAPTER V

### ACTIVATED CARBON MONOLITH WITH HIERARCHICAL POROUS STRUCTURE PREPAED BY DIRECT THERMAL AND CHEMICAL ACTIVATION

The carbonized RF monolithic gel or carbon monolith with interconnected macropores in the different sizes, which can easily be adjusted by changing the synthesis parameters at the gel-formation step such as initial pH, temperature and ultrasonic power, are introduced in previous chapter. However, the obtained porous structure of the carbon monoliths give only in the micropores that is not suitable for some applications. The porous structure in the range of mesopores and the chemical surface groups mainly consisting of oxygenated functional groups, therefore, are necessarily generated in the carbon monolith. In this chapter the simple procedure to improve the both mesoporous structure and oxygenated functional groups in the activated carbon monolith consisting of the interconnected macroporous structure is the aim of this study. The study is focused on the direct thermal activation with  $\text{CO}_2$  and the direct chemical activation of the RF monolith gel. The direct thermal activation is carried out by directly activating the RF monolith gel that the carbonization is not needed for treatment before. While the direct chemical activation is performed by impregnation of  $\text{Ca}(\text{NO}_3)_2$  into the RF monolith gel and followed by directly activating with  $\text{CO}_2$ .

The influence of the main parameters, activation temperature and time, on the obtained porous structure and oxygenated functional groups of both direct thermal activation and direct chemical activation are mainly emphasized here. Moreover, the comparison of the hierarchical porous structure and the oxygenated functional groups of the hierarchical porous carbon monoliths prepared from carbonization with  $\text{N}_2$ , direct thermal activation and direct chemical activation are discussed also.

## 5.1 Experimental

All of RF monolithic gels which used to prepare carbon monolith in this experimental are prepared under the synthesis condition of s-C4 as shown in Table 4.1 at section 4.1.1.

### 5.1.1 Carbonization with N<sub>2</sub>

For the carbonization, the RF dried-monolith gel was carbonized with N<sub>2</sub> gas flow of 50 cm<sup>3</sup>(at STP)/min in a quartz tube reactor at a heating rate of 10 °C /min ,until the desired temperature, T<sub>D</sub>, was reached and followed by maintaining the keeping time for 30 min.

### 5.1.2 Direct thermal activation with CO<sub>2</sub>

For the direct thermal activation, the RF dried-monolith gels were conducted by thermal activation with CO<sub>2</sub> gas flow of 50 cm<sup>3</sup>(at STP)/min in a quartz tube reactor at a heating rate of 10 °C /min until the desired temperature, T<sub>D</sub>, was reached and followed by maintaining the keeping time for 30 min. The operating conditions are shown in Table 5.1 as c-C1 to c-C4.

### 5.1.3 Direct chemical activation

Firstly, the RF dried-monolith gels were soaked into the solution of 0.4 M of Ca(NO<sub>3</sub>)<sub>2</sub> for 3 days and stirring with magnetic stirrer during all time. After that, the wetted-Ca(NO<sub>3</sub>)<sub>2</sub> RF monolith gels were dried at 75 °C until their weight was constant. Thermal activation was conducted in a quartz tube reactor with CO<sub>2</sub> flow at 50 cm<sup>3</sup> (at STP) /min. The reactor was heated at the heating rate of 10 °C /min until the temperature reached the desired temperature, T<sub>D</sub>, as shown in Table 5.1, and then they were kept at this temperature for 30 min. The temperature, then, was cooled down to the room temperature. Finally the activated carbon monoliths were obtained.

### 5.1.4 Characterizations

The porous structure in monolithic forms of both RF gels and carbons are revealed by scanning electron microscope (JEOL, JSM-6700F). The macropore size

distribution of the macroporous monolithic carbon is obtained by mercury porosimeter (Micromeritics, Pore-Sizer-9320).

The micro- / mesopores are determined from the adsorption and desorption isotherms of  $N_2$  at 77 K measured by adsorption apparatus (BEL, mini-BEL Sorp.). According to IUPAC classification, pores can be divided into three categories depending on their sizes: micropores ( $\leq 2$  nm), mesopores (2 – 50 nm) and macropores ( $\geq 50$  nm). The definition of micropores and mesopores introduced by IUPAC was adopted. Then, the micropore volume,  $V_{\text{micro}}$ , was determined by t-plot while the mesopore volume and mesopore size distribution were derived from Dollimore-Heal method [43]. For the specific surface area,  $S_{\text{sp}}$ , is obtained from an average values between the Brunauer-Emmett-Teller (BET) specific surface area,  $S_{\text{BET}}$ , and the t-plot specific surface area,  $S_{\text{t-plot}}$ , that they were usually applied to determine the specific surface area of the activated carbon [44], and were derived from BET model and t-plot model, respectively.

A decrease in weight of the obtained carbon monoliths, % burn-off, was measured after carbonization and both physical and chemical activations. Fourier Transform Infrared (FTIR) spectra were recorded using spectrometer (Perkin Elmer, 1615), and the samples for analysis is formed as pellets made by crushing and mixing the samples with spectroscopy grade of KBr.

Table 5.1: Synthesis conditions of the activated carbon monoliths

Sample	Conditions of carbon synthesis				
	Carbonization with N <sub>2</sub>	Direct thermal activation with CO <sub>2</sub>	Direct chemical activation with Ca(NO <sub>3</sub> ) <sub>2</sub> -CO <sub>2</sub>	T <sub>D</sub> [°C]	t <sub>D</sub> [min]
	<b><u>Carbonization with N<sub>2</sub></u></b>				
n-C	Yes	-	-	850	30
	<b><u>Direct thermal activation at various temperature</u></b>				
c-C1	-	Yes	-	700	30
c-C2	-	Yes	-	800	30
c-C3	-	Yes	-	850	30
c-C4	-	Yes	-	900	30
	<b><u>Direct chemical activation at various temperature</u></b>				
ca-C1	-	-	Yes	500	30
ca-C2	-	-	Yes	700	30
ca-C3	-	-	Yes	800	30
ca-C4	-	-	Yes	850	30
ca-C5	-	-	Yes	900	30
	<b><u>Direct chemical activation at various time</u></b>				
ca-C6	-	-	Yes	800	15
ca-C7	-	-	Yes	800	30
ca-C8	-	-	Yes	800	60
ca-C9	-	-	Yes	800	90
ca-C10	-	-	Yes	800	120

## 5.2 Results and discussion

### 5.2.1 Activated carbon monolith consisting with bimodal hierarchical pores prepared from direct thermal activation with CO<sub>2</sub>

Table 5.2: Porous properties of the macroporous carbon monoliths prepared by various activation methods

Samples	% Burn-off	Type of Isotherm	Pore volume [cm <sup>3</sup> /g]		$S_{sp}$ [m <sup>2</sup> /g]	Final form
			$V_{micro}$	$V_{meso}$		
c-C1	41	I	0.15	*ND	420 ± 75	Monolith
c-C2	49	I	0.20	ND	634 ± 92	Monolith
c-C3	55	I	0.23	ND	752 ± 55	Monolith
c-C4	71	I	0.37	ND	968 ± 113	Monolith

Remark: \*ND = not determined

The direct thermal activation process under CO<sub>2</sub> gas is performed in the range of activation temperature,  $T_D$ , between 700 °C to 900 °C, and the heating rate and the activation time are fixed at 10 °C/min and 30 min, respectively. After processing, the monolith structure, as shown in Figure 5.1 (a), of the activated carbons is maintained as well as the RF monolith gels. The macroporous structure of the activated carbon monoliths derived from the activation temperature of 700 °C, 800 °C and 850 °C are presented by scanning electro microscope (SEM) images as shown in Figure 5.1 (b), (c) and (d), respectively. They confirm that the interconnected macroporous structure can be maintained in these activated carbon monoliths. In order to confirm that this activation process is available to produce the carbon monolith with hierarchical porous structure, the existences of either micropores or mesopores in the interconnected macropores of these carbon monoliths are continuously considered.

Considering to the adsorption-desorption isotherms of N<sub>2</sub> at 77 K at Figure 5.2, It is used to describe the textural porosities, in particular micropores and mesopores, of the activated carbon monoliths. Here the amount of N<sub>2</sub> adsorbed,  $V$ , is plotted against the relative pressure,  $p/p_0$ , of N<sub>2</sub>. One can see that the amount of N<sub>2</sub> increase with increasing of the activation temperature,  $T_D$ ,

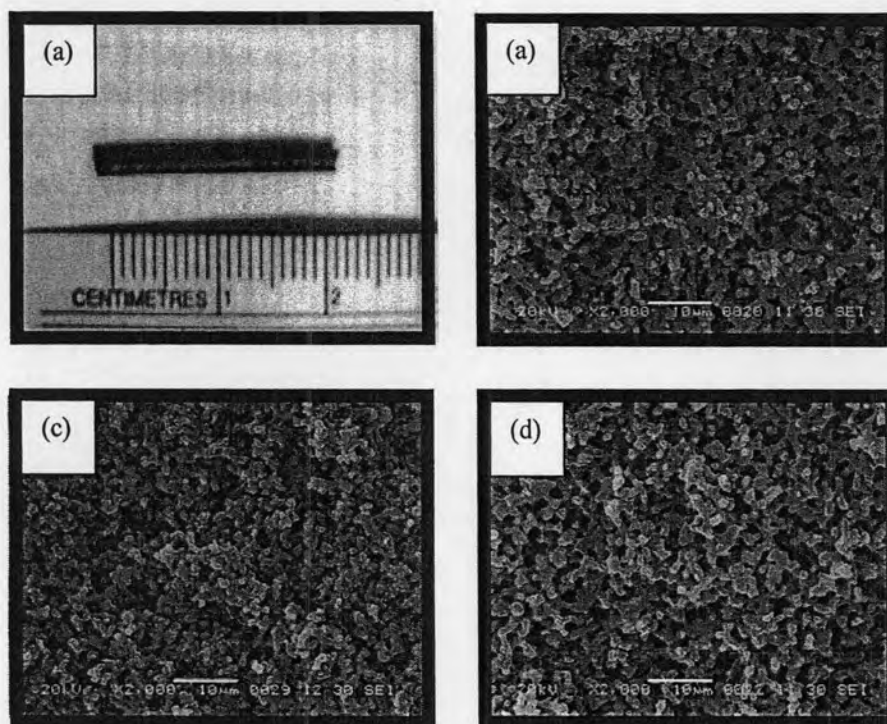


Figure 5.1: (a) Photograph of the activated carbon monoliths prepared from direct thermal activation and (b) – (d) SEM images of the macroporous structure of (b) c-C1, (c) c-C3 and (d) c-C4.

---

It seems to indicate that the porosities are developed increasingly with elevating  $T_D$ . In addition, the isotherms according to the IUPAC classification are Type-I at all, which indicates that the microporous structure decorated on the interconnected macroporous structure of the activated carbon monoliths are the micropores in nature and the absence of significant mesoporous structure. This result indicates that the activated carbon monoliths consisting of the microporous structure on the interconnected macropores can be prepared by the processing of direct thermal activation with  $\text{CO}_2$ .

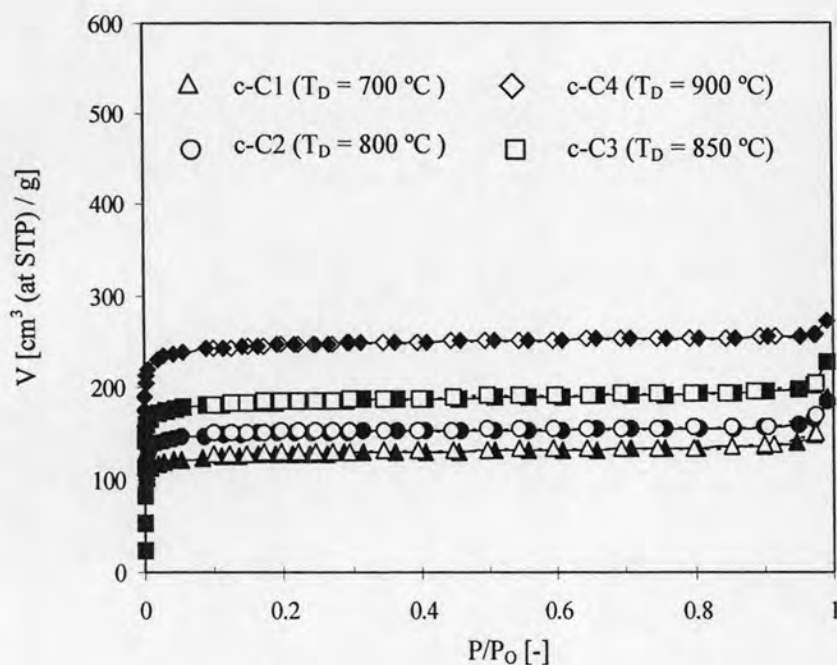


Figure 5.2: N<sub>2</sub> adsorption-desorption isotherms at 77 K the activated carbon monoliths prepared from direct thermal activation with CO<sub>2</sub>.

The characteristics of the microporosity consisting with the micropore volume,  $V_{\text{micro}}$ , and the specific surface area,  $S_{\text{sp}}$ , of the activated carbon monoliths can be determined from the N<sub>2</sub> adsorption-desorption isotherms. According to Table 5.2, it suggests that  $V_{\text{micro}}$  of the activated carbon monoliths prepared from  $T_D$  of 700 °C, 800 °C, 850 °C and 900 °C are 0.15, 0.20, 0.23 and 0.37 cm<sup>3</sup>/g, respectively, whereas  $V_{\text{meso}}$  cannot be detected from these isotherms. It is obviously noticed that the increasing amount of  $V_{\text{micro}}$  in the activated carbon monoliths is depended drastically on an increase of  $T_D$  as shown in Figure 5.3 (a).

The specific surface area,  $S_{\text{sp}}$ , of the activated carbon monoliths prepared under  $T_D$  of 700 °C, 800 °C, 850 °C and 900 °C are  $420 \pm 75$ ,  $634 \pm 92$ ,  $752 \pm 55$  and  $968 \pm 113$  m<sup>2</sup>/g, respectively, as presented in Table 5.3. The incremental trend of  $S_{\text{sp}}$  against to  $T_D$  is shown in Figure 5.3 (b). Both increasing of  $V_{\text{micro}}$  and  $S_{\text{sp}}$  can be confirmed in microporosity in the interconnected macroporous structure of the activated carbon monoliths with an increase of activation temperature.

The % burn-off of the activated carbon monoliths derived from  $T_D$  of 700 °C, 800 °C, 850 °C and 900 °C are 41%, 49%, 55% and 71%wt, respectively, as shown in

Table 5.3. Their increasing with  $T_D$  corresponds with more development of the microporosities.

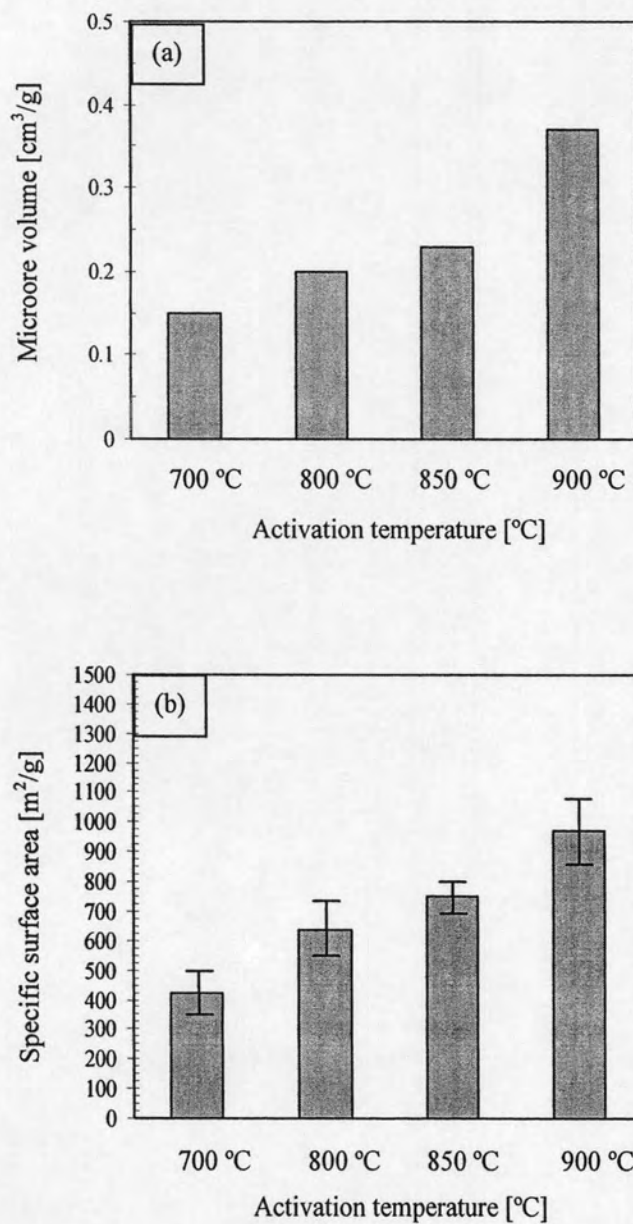


Figure 5.3: (a) Micropore volume and (b) specific surface area of the activated carbon monolith prepared by direct thermal activation with  $\text{CO}_2$  at various activation temperatures.



### 5.2.2 Activated carbon monolith consisting with tri-modal hierarchical porous structure prepared by direct chemical activation

Table 5.3: Porous properties of the activated carbon monoliths prepared by various activating conditions

Samples	% Burn-off	Type of Isotherm	Pore volume [cm <sup>3</sup> /g]		$S_{sp}$ [m <sup>2</sup> /g]	Final form
			$V_{micro}$	$V_{meso}$		
<b><u>Effect of activation temperature</u></b>						
ca-C1	38	I	0.08	ND	255 ± 40	Monolith
ca-C2	51	I	0.18	ND	547 ± 80	Monolith
ca-C3**	65	IV + I	0.20	0.25	663 ± 71	Monolith
ca-C4	71	IV + I	0.22	0.38	811 ± 80	Monolith
ca-C5	78	IV + I	0.34	0.28	995 ± 99	Cracking
<b><u>Effect of activation time</u></b>						
ca-C6	61	IV + I	0.17	0.11	636 ± 69	Monolith
ca-C7**	65	IV + I	0.20	0.25	663 ± 80	Monolith
ca-C8	70	IV + I	0.30	0.29	706 ± 68	Monolith
ca-C9	77	IV + I	0.31	0.38	816 ± 80	Monolith
ca-C10	82	IV + I	0.31	0.44	935 ± 153	Cracking

Remark: \*ND = not determined

\*\*ca-C3 and ca-C7 are same

A direct chemical activation process for preparing the activated carbon monoliths performed by loading  $\text{Ca}(\text{NO}_3)_2$  into the interconnected macroporous RF monolith gel, and followed by the activation with  $\text{CO}_2$  is investigated and presented in this work. The operating conditions consisting of the activation temperature,  $T_D$ , and time,  $t_D$ , are confined to study in the range between 500 °C to 900 °C (at constant  $t_D = 30$  min) and 15 to 120 min (at constant  $T_D = 800$  °C), respectively. The obtainable monolith form of the activated carbons is depended on both  $T_D$  and  $t_D$ . Table 5.3 shows that the activated carbon in monolith form cannot be maintained when  $T_D$  and  $t_D$  reach to 900 C° and 120 min, respectively. Figure 5.4 (a), (b), (c) and (d) show SEM images of the interconnected macroporous structure of the activated carbon monoliths denoted as ca-C3 ( $T_D$  at 800 °C,  $t_D$  at 30min), ca-C4 ( $T_D$  at 850 °C,  $t_D$  at 30min), ca-C8 ( $T_D$  at 800 °C,  $t_D$  at 60min), and ca-C9 ( $T_D$  at 800 °C,  $t_D$  at 90 min) in

Table 5.3, respectively. These results confirm that the interconnected macroporous structure can be maintained.

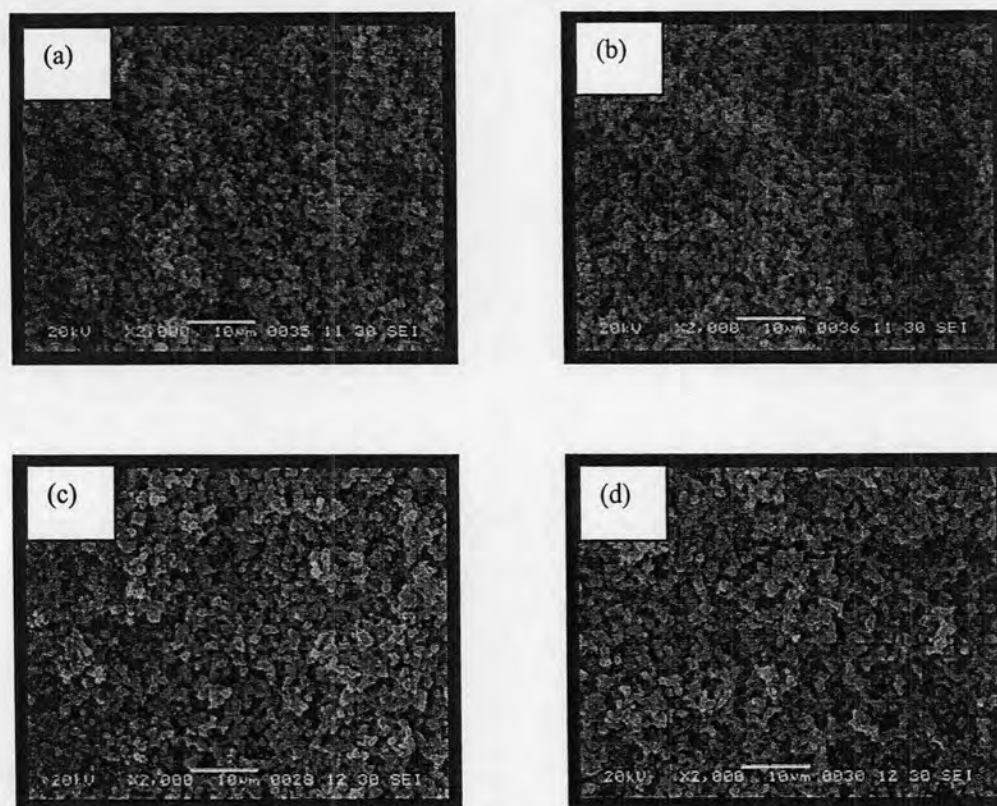


Figure 5.4: Macroporous structure of the activated carbon monolith prepared by direct chemical activation process at different activation temperature and time; (a) ca-C3, (b) ca-C4, (c) ca-C8 and (d) ca-C9.

#### *Role of activation temperature evolution of the micro-/ and mesoporous structure*

Figure 5.5 shows the adsorption-desorption isotherms of  $N_2$  at 77 K on the activated carbon monoliths, ca-C1, ca-C2, ca-C3, ca-C4 and ca-C5, which obtained from RF monolith gels by wet impregnated with  $Ca(NO_3)_2$  in their structure and directly followed activation with  $CO_2$  for 30 min under different activating temperatures,  $T_D$ , as shown in Table 5.3. From the isotherms of ca-C3, ca-C4 and ca-C5, the combination forms of type I and type IV isotherms, classification by IUPAC, are shown with H3 hysteresis loop.

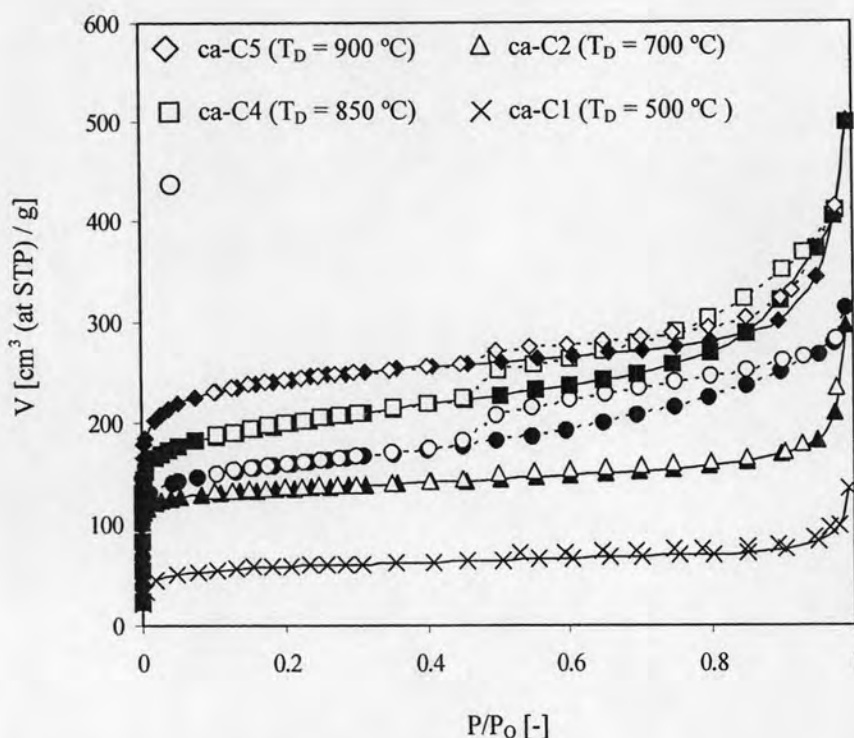


Figure 5.5:  $N_2$  adsorption-desorption isotherms at 77 K of the carbon monoliths prepared by direct chemical activation at various activation temperature,  $T_D$ .

It can be implied that these samples have both micropores and slit-pore shape of mesopores, therefore the mesopore size distributions cannot be defined accurately [45]. Meanwhile, ca-C1 and ca-C2 exhibit only type I isotherm which means that only microporous structure are presented.

The micropore volume,  $V_{\text{micro}}$ , mesopore volume,  $V_{\text{meso}}$ , and specific surface area,  $S_{\text{sp}}$ , in Table 5.3 are determined from the  $N_2$  adsorption-desorption as shown in Figure 5.5. The  $V_{\text{mic}}$  of ca-C1, ca-C2, ca-C3, ca-C4 and ca-C5 are 0.08, 0.18, 0.20, 0.22 and 0.34  $\text{cm}^3/\text{g}$ , respectively. It is obvious that an increase in  $V_{\text{mic}}$  and  $S_{\text{sp}}$  are resulted in an increase in  $T_D$ , as shown in Figure 5.6 and Figure 5.7, respectively. The  $V_{\text{meso}}$ , of ca-C3, ca-C4 and ca-C5 as shown in Table 5.3 are 0.25, 0.38 and 0.28  $\text{cm}^3/\text{g}$ , respectively, whereas the  $V_{\text{meso}}$  of ca-C1 and ca-C2 cannot be obtained. In addition, the mesopore size distributions as shown in Figure 5.8 suggest that the pore radiuses are also larger and wider when  $T_D$  increases.

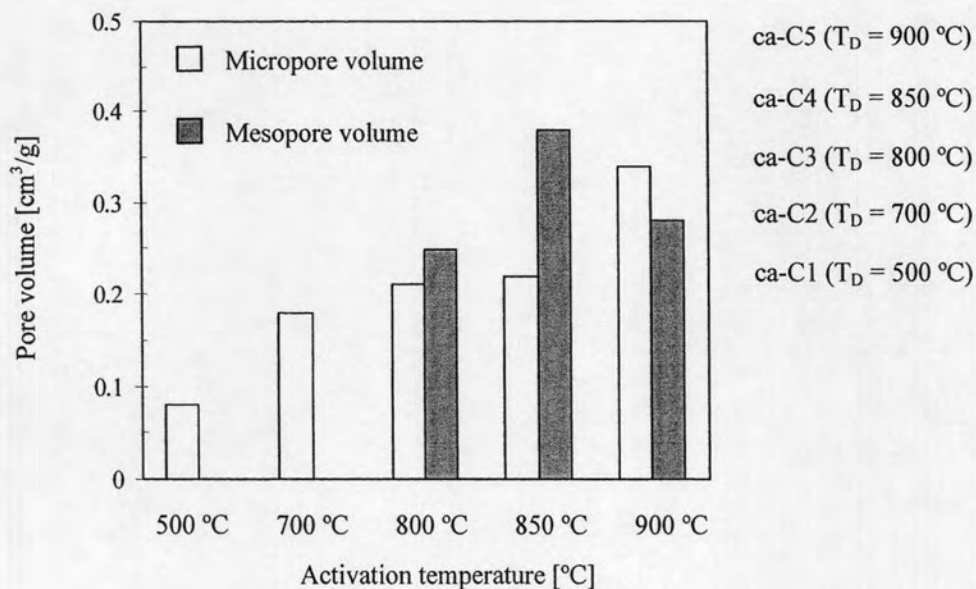


Figure 5.6: Comparing micro-/ and mesopore volume of the carbon monoliths prepared by direct chemical activation at various activation temperature,  $T_D$ .

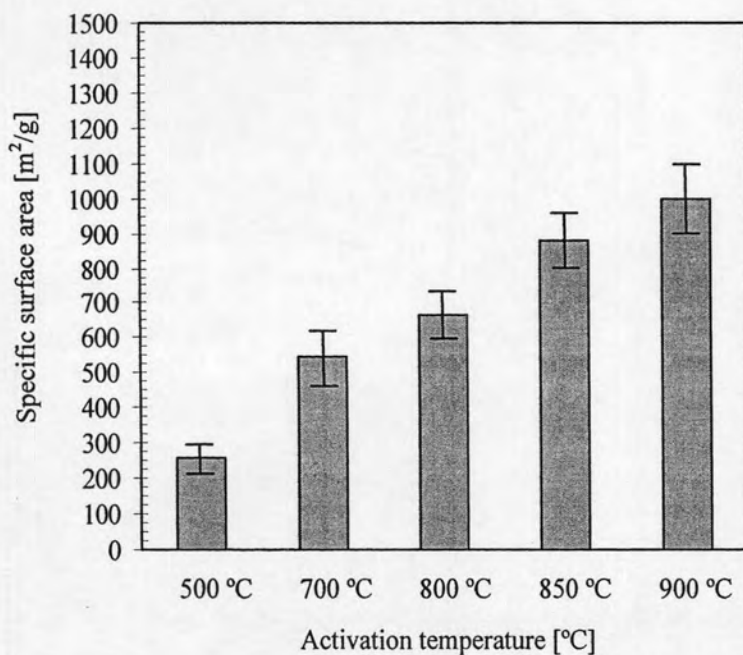


Figure 5.7: Specific surface area of the activated carbon monoliths prepared by direct chemical activation at various activation temperature,  $T_D$ .

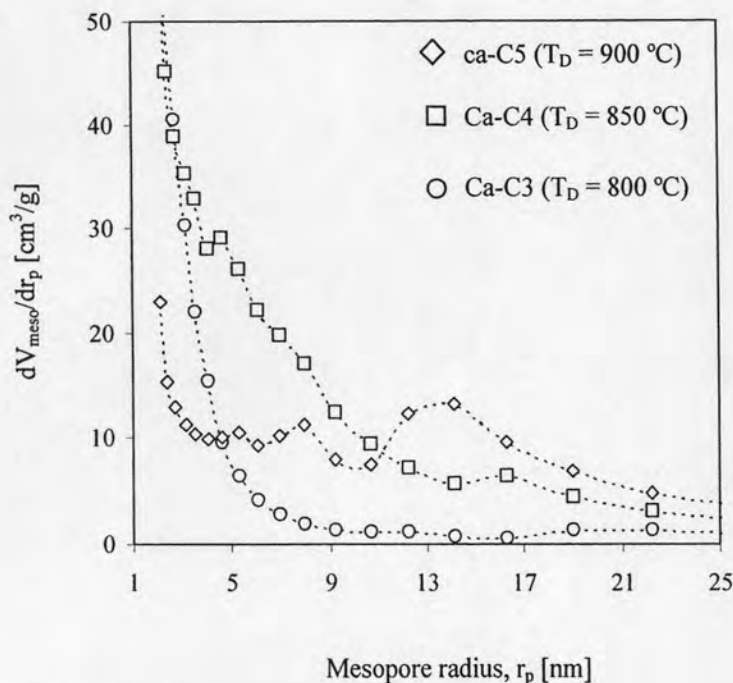


Figure 5.8: The mesopore size distributions of the activated carbon monoliths prepared by direct chemical activation at various activation temperature,  $T_D$ .

The results indicate that the mesopore volume can be generated when  $T_D$  reaches 800 °C, and it can continuously be developed until  $T_D$  increasing to 850 °C. However, the mesopore volume decreases when  $T_D$  reaches 900 °C.

The % burn-off as shown in Table 5.3 for ca-C1, ca-C2, ca-C3, ca-C4 and ca-C5 are 38 %, 51 %, 65 %, 71 % and 78 %wt, respectively. One can see that the % burn-off values correspond with the development of micro- and mesoporosity in the carbon monoliths.

#### *Role of activation temperature evolution of the micro-/ and mesoporous structure*

Figure 5.9 shows the adsorption-desorption of  $N_2$  at 77 K on the activated carbon monoliths, ca-C6, ca-C7, ca-C8, ca-C9 and ca-C10, which obtained from RF monolith gels by wet impregnated with  $Ca(NO_3)_2$  in their structure and directly followed activation with  $CO_2$  at 800 °C under different activating time,  $t_D$ , as shown in Table 5.3. It can be noticed that all isotherms are the combinations of Type I and IV

with H3 hysteresis loop. Therefore, it is confirmed that the micropores and slit-shape mesopores are located in the interconnected macroporous structure of the activated carbon monoliths.

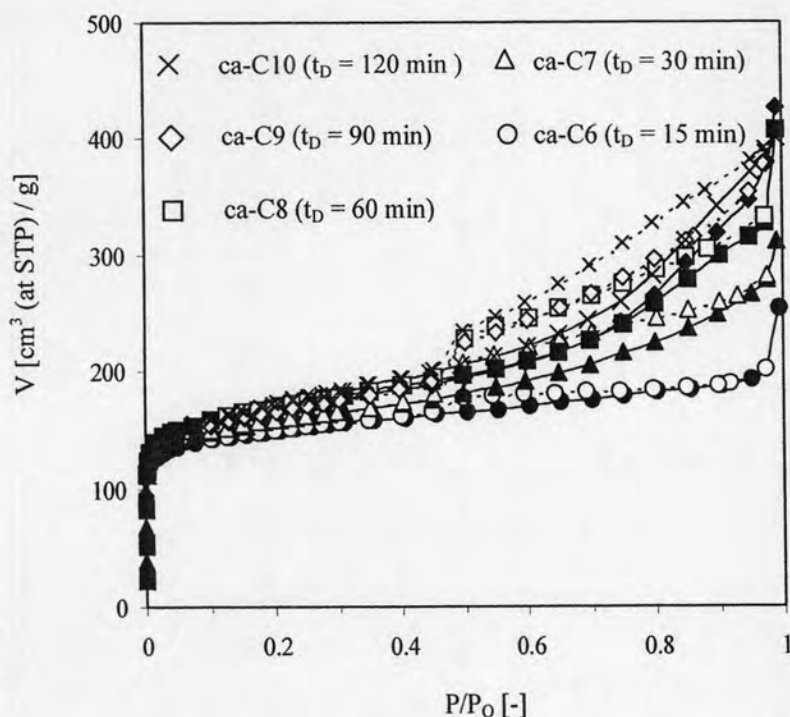


Figure 5.9:  $N_2$  adsorption-desorption isotherms at 77 K of the carbon monoliths prepared by direct chemical activation at various activation time,  $t_D$ .

The micropore volume,  $V_{\text{micro}}$ , as shown in Table 5.3 are 0.17, 0.20, 0.30, 0.31 and  $0.31 \text{ cm}^3/\text{g}$  for ca-C6, ca-C7, ca-C8, ca-C9 and ca-C10, respectively. The results as shown in Figure 5.10 obviously indicate that the  $V_{\text{micro}}$  are increasingly developed with increasing  $t_D$ , and becomes constant at the value of  $0.31 \text{ cm}^3/\text{g}$  at 60 min activation time.

As for the development of the mesopore volume,  $V_{\text{meso}}$ , as shown in Table 5.3 are 0.11, 0.25, 0.29, 0.38 and  $0.44 \text{ cm}^3/\text{g}$  for ca-C6, ca-C7, ca-C8, ca-C9 and ca-C10. The results indicate that the  $V_{\text{meso}}$  are increasingly developed with increasing  $t_D$ . However, the activation time must be shorter than 120 min in order to obtain the activated carbon in monolith shape.

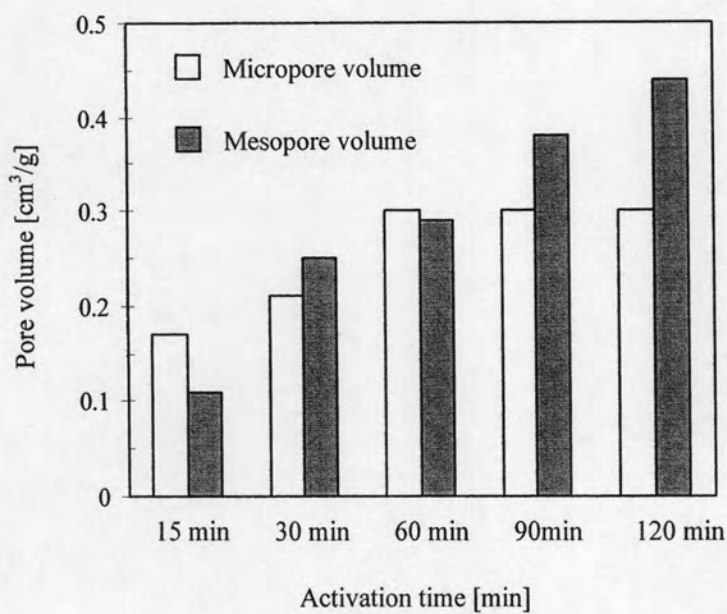


Figure 5.10: Micro- and mesopore volume of the carbon monoliths prepared by direct chemical activation at various activation time,  $t_D$ .

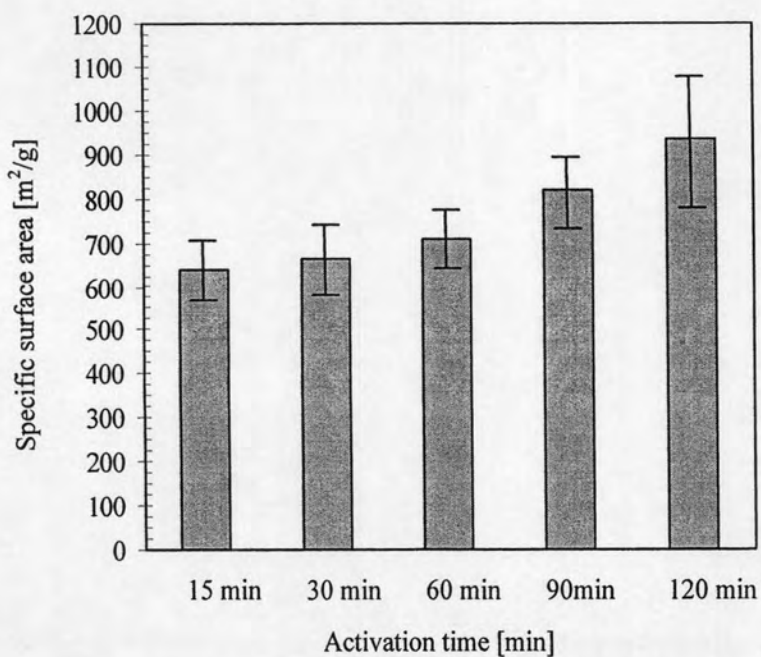


Figure 5.11: Specific surface area of the activated carbon monoliths prepared by direct chemical activation at various activation time,  $t_D$ .

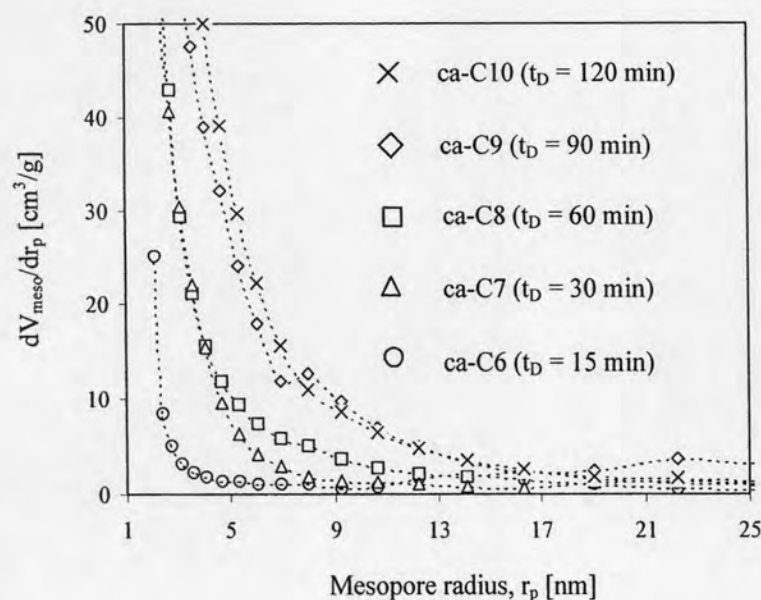


Figure 5.12: Mesopore size distributions of the activated carbon monoliths prepared by direct chemical activation at various activation time,  $t_D$ .

### 5.2.3 The effect of different heat treatments on hierarchical porous structure of the carbon monolith

Table 5.4: Porous properties of the macroporous carbon monoliths prepared by various heat treatments methods

Samples	% Burn-off	Type of Isotherm	Pore volume [cm <sup>3</sup> /g]		$S_{sp}$ [m <sup>2</sup> /g]	Final form
			$V_{micro}$	$V_{meso}$		
n-C	54	I	0.20	*ND	750 ± 99	Monolith
c-C3	55	I	0.23	ND	752 ± 55	Monolith
ca-C4	71	IV+I	0.22	0.38	811 ± 80	Monolith

Remark: \*ND = not determined

The influences of carbonization with  $N_2$ , thermal activation with  $CO_2$  and  $Ca(NO_3)_2$ -impregnated followed by thermal activation with  $CO_2$  on the micro-/mesoporosities of the carbon monolith are studied on n-C, c-C3 and ca-C4, respectively. The preparation conditions are shown in Table 5.1.



The SEM micrographs in Figure 5.13 (a), (b) and (c) which show the interconnected macroporous structure in the carbon monoliths of n-C, c-C3 and ca-C4 respectively suggest that the interconnected macroporous structure of the carbon monolith can be maintained in these samples. The macropore size distributions of these samples, as shown in Figure 5.13 (d), are slightly different. In addition, the macropore volume of ca-C4 ( $0.91 \text{ cm}^3/\text{g}$ ) is smaller than n-C ( $1.00 \text{ cm}^3/\text{g}$ ) and c-C3 ( $0.98 \text{ cm}^3/\text{g}$ ).

From the isotherms of n-C and c-C3 as shown in Figure 5.14, they are classified by IUPAC as type I which means that these samples have only the micropores on the macroporous wall of its monolithic shape. Whereas the isotherm of ca-C4 as shown in Figure 5.14 exhibits in combination of type I and type IV with H3 hysteresis loop which indicates that the sample has micropores, slit-pore shape of mesopores and not well-defined mesopore size distribution [45].

According to Table 5.4, it suggests that there are only microporous structure on n-C and c-C3 (micropore volume,  $V_{\text{mic}}$ , =  $0.20$  and  $0.23 \text{ cm}^3/\text{g}$ , respectively) while the mesoporous and microporous structure appear on ca-C4 (mesopore volume,  $V_{\text{mes}}$ , =  $0.38 \text{ cm}^3/\text{g}$  and micropore volume,  $V_{\text{mic}}$ , =  $0.22 \text{ cm}^3/\text{g}$ ). The specific surface area,  $S_{\text{sp}}$ , of ca-C4 ( $811 \pm 80 \text{ m}^2/\text{g}$ ) is much larger than n-C and c-C3 ( $750 \pm 99 \text{ m}^2/\text{g}$  and  $752 \pm 55 \text{ m}^2/\text{g}$ ) as a result of additional mesopores. In order to % burn-off for n-C, c-C3 and ca-C4 are 54 %, 55 % and 71 %, respectively. They correspond reasonably with the development of micro- and mesoporosity of the carbon monoliths.

These results indicate that the micropores on the interconnected macroporous carbon monolith can be created by either carbonization with  $\text{N}_2$  or direct thermal activation with  $\text{CO}_2$  at  $850 \text{ }^\circ\text{C}$ , whereas the presence of  $\text{Ca}(\text{NO}_3)_2$  in the structure of the RF monolith gel is needed to generate mesopores on the interconnected macroporous carbon monolith

The rate of activation of the  $\text{CO}_2$ -thermal activation with and without  $\text{Ca}(\text{NO}_3)_2$ -loaded can be evaluated from the slope in the linear regions of the plot between % burn-off and time as shown in Figure 5.15. The calculated rate of the  $\text{CO}_2$ -thermal activation of c-C3 and ca-C4 are 7.2% and 11.9 %wt /hr, respectively. It is clear that the presence of  $\text{Ca}(\text{NO}_3)_2$  in the RF monolith gel can act as an effective catalyst in the  $\text{CO}_2$ -thermal activation process.

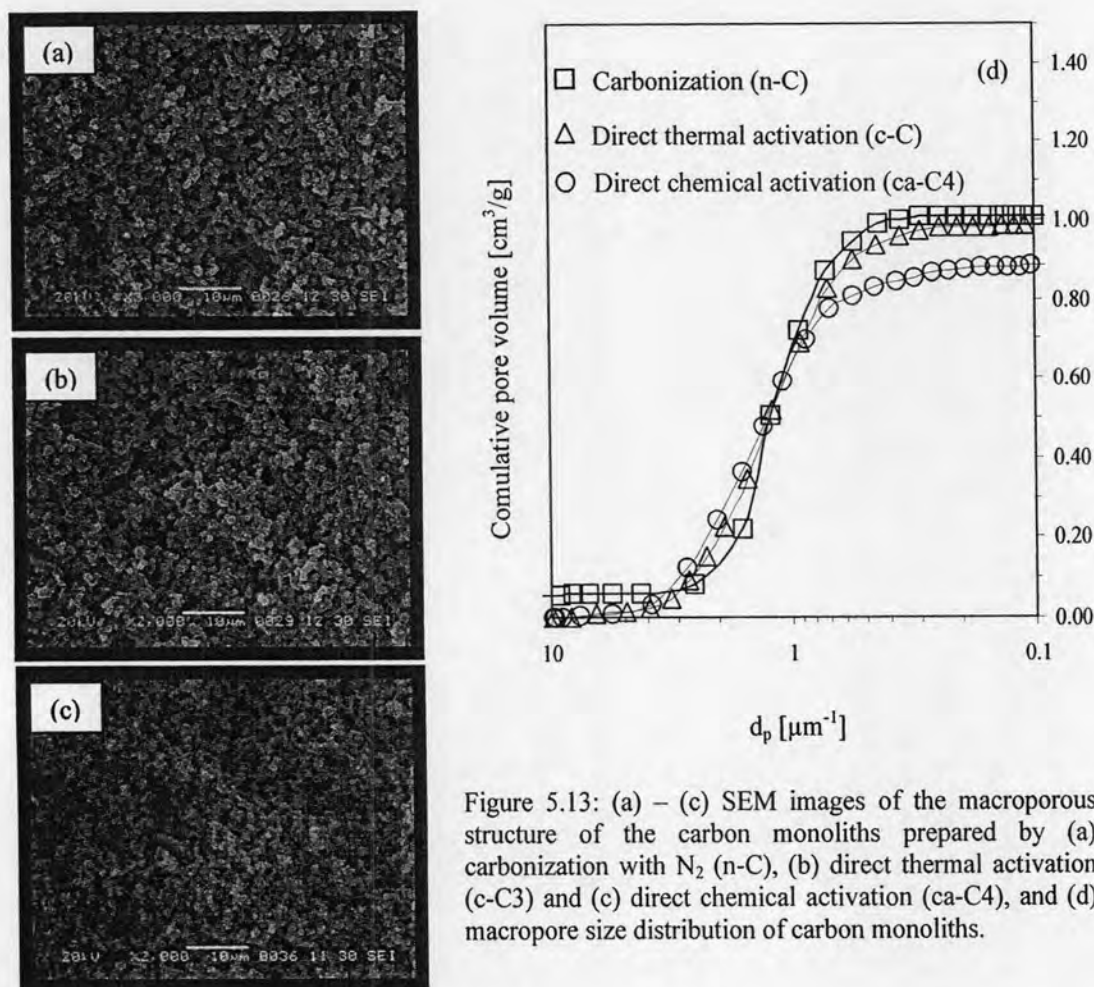


Figure 5.13: (a) – (c) SEM images of the macroporous structure of the carbon monoliths prepared by (a) carbonization with N<sub>2</sub> (n-C), (b) direct thermal activation (c-C3) and (c) direct chemical activation (ca-C4), and (d) macropore size distribution of carbon monoliths.

In summary, the results from this work suggest that the activated carbon monolith with hierarchical porous structure can be synthesized, without using templates, by both direct thermal activation process and direct chemical activation processes of the interconnected macroporous RF monolith gel, which is synthesized by sol-gel reaction assisted by ultrasonic irradiation. The activated carbon monolith prepared by the direct thermal activation process consists with the hierarchical bimodal micro-/macropores within the internal structure, whereas the activated carbon monolith prepared by another process consists with the hierarchical tri-modal micro-/meso-/ macropores in its structure. Moreover, the activating time for both activations is short ( $\sim 30$  to  $60$  min) for producing the activated carbon monolith with high surface area ( $\sim 700$  m<sup>2</sup>/g at the temperature of 850 °C).

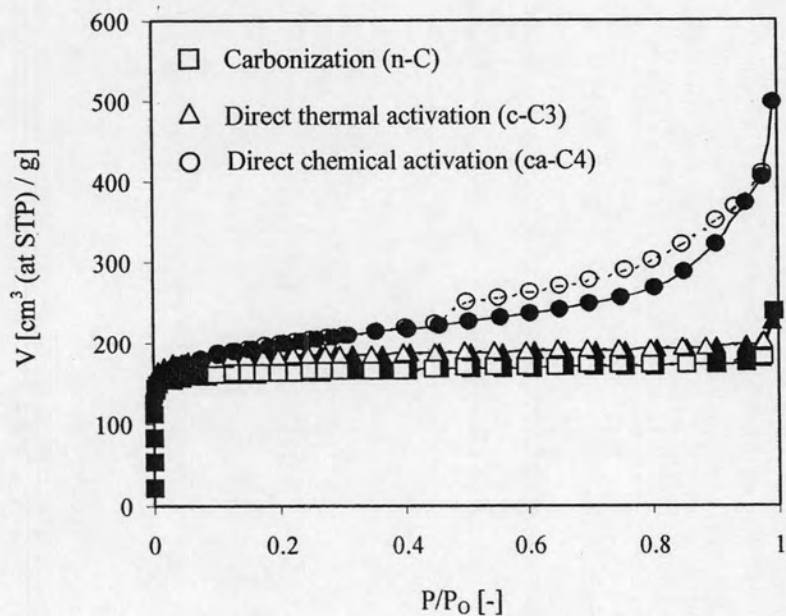


Figure 5.14: N<sub>2</sub> adsorption-desorption isotherms at 77 K of the carbon monoliths prepared by carbonization with N<sub>2</sub> (n-C), direct thermal activation with CO<sub>2</sub> (c-C3) and direct chemical activation (ca-C4).

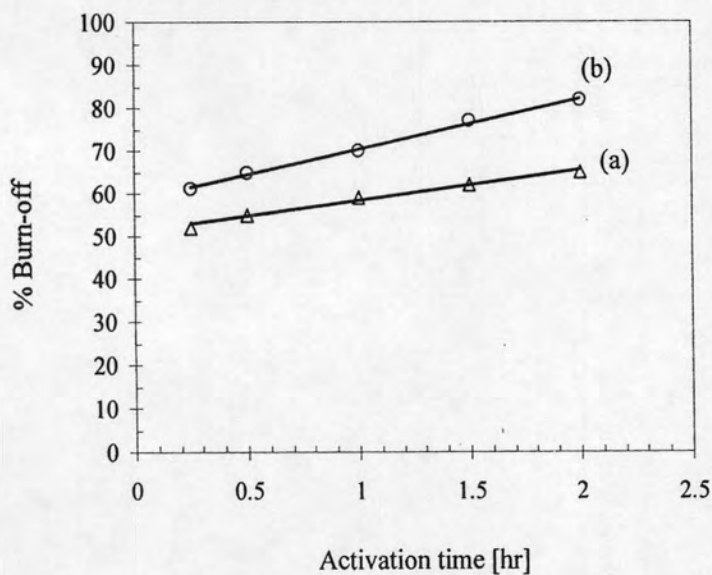


Figure 5.15: %Burn-off as a function of time of the activated carbon monoliths prepared by carbonization with N<sub>2</sub> (n-C), direct thermal activation with CO<sub>2</sub> (c-C3) and direct chemical activation (ca-C4).

#### 5.2.4 Oxygenated functional groups in the activated carbon monoliths

In many applications of the activated carbon, the existence of both high specific surface area and high porosity are not their only promising characteristics, but also their oxygenated surface functional groups [47, 53, 68-72]. Oxygen in surface functional groups of the activated carbons can be found in the form of various functional groups bonding at the edges of the basal plane (polyaromatic system). These functionalities are generally separated into two families depend on their acidic or basic character in aqueous solution [41, 47]. On one hand, carboxyl, anhydrides, lactones, phenol, and lactol groups account for the acidic character of the activated carbon. On the other hand, cyclic ketones, cyclic ether, and pyrone groups are the basic functionalities.

The aims of this section are focused on oxygenate functionality analyzed from FT-IR spectrum of the activated carbon monoliths, which are obtained from direct thermal and chemical activation with  $\text{CO}_2$ . Moreover, an investigation on the development of oxygenated functional groups of the activated carbon monoliths prepared by different activation temperature is presented.

Prior to an investigation on FT-IR results, the significant peaks of surface functional groups in the activated carbons which have been studied by many authors are briefly introduced and shown in Table 5.5. These interpretations will be used as a guideline for an analysis of the surface functional groups in the activated carbons, which are prepared from carbonization with  $\text{N}_2$ , direct thermal activation and direct chemical activation in this work.

Table 5.5: Implication of infrared spectrum peaks for interpretation on surface functional groups of activated carbons.

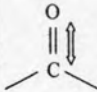
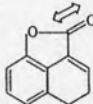
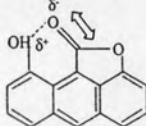
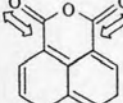
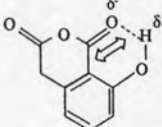
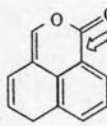
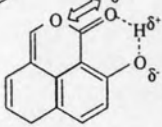
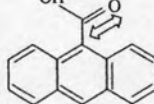
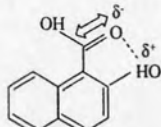

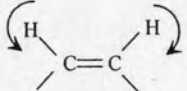
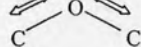
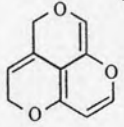
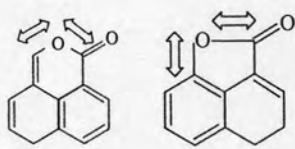
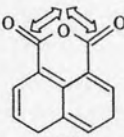
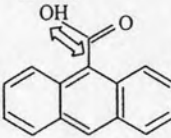
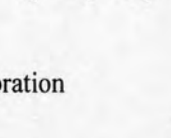
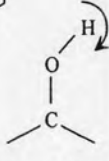
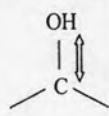
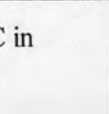
IR peak bands [cm <sup>-1</sup> ]	Implications	References
~ 3200 - 3600	<p>Corresponding to functional groups involved in H-bonding (N-H, O-H)</p> <p>~ 3400 cm<sup>-1</sup>: corresponding with hydroxyl groups (-OH)</p> <p>~ 3600 cm<sup>-1</sup>: corresponding with amine groups (-NH)</p>	[40-42]
~ 1650 - 1850	<p> Corresponding to the functional groups consisting of the bonding C=O vibrations</p> <p>~ 1830 cm<sup>-1</sup>: five-membered ring lactone </p> <p>~ 1737 cm<sup>-1</sup>: five-membered ring lactone induced by hydroxyl groups </p> <p>~ 1810 - 1740 cm<sup>-1</sup>: aldehyde </p> <p>~ 1770 - 1670 cm<sup>-1</sup>: aldehyde induced by hydroxyl groups </p> <p>~ 1790 cm<sup>-1</sup>: six-membered ring lactone </p> <p>~ 1711 cm<sup>-1</sup>: six-membered ring lactone induced by hydroxyl groups </p> <p>~ 1750 cm<sup>-1</sup>: carboxyl group </p> <p>~ 1660 - 1700 cm<sup>-1</sup>: carboxyl group induced by hydroxyl groups </p>	[42, 47-57]

Table 5.5 (next): Implication of infrared spectrum peaks for interpretation on surface functional groups of activated carbons

IR peak bands [cm <sup>-1</sup> ]	Implications	References
~ 1550 - 1650	Corresponding with C=C stretching vibration modes of the basal plane of activated carbons 	[41, 42, 47-57]
~1350 - 1550	Corresponding to C-H bending vibration mode in basal plane 	[51, 52, 56, 57]
~ 1000 - 1300	Corresponding to C-O stretching vibration modes  ~ 1025 - 1141 cm <sup>-1</sup> : cyclic ether group  ~1230 - 1250 cm <sup>-1</sup> : ether bridge between rings  ~ 1160 - 1370 cm <sup>-1</sup> : C-O in lactone  ~ 980 - 1300 cm <sup>-1</sup> : C-O in aldehyde  ~ 1120 - 1200 cm <sup>-1</sup> : C-O in carboxyl  ~ 1160 - 1200 cm <sup>-1</sup> : C-O-H bending vibration  ~ 1000 - 1220 cm <sup>-1</sup> : C-OH stretching vibration 	[47, 51-53, 56-57]
< 900	Corresponding to out-of-plane bending vibration of C-C in the basal plane of the activated carbon 	[54, 56]

*Oxygenated surface functional groups of carbon monoliths prepared by carbonization, direct thermal activation and direct chemical activation*

The infrared spectra of carbon monoliths prepared by carbonization with  $N_2$  (n-C), direct thermal activation with  $CO_2$  (c-C3) and direct chemical activation (ca-C4), respectively, are shown in Figure 5.16 (a), (b) and (c), respectively. The prepared conditions are shown in Table 5.1.

For the mainly functional groups of the RF monolith gel, it has been discussed in the section 4.2.1.3 that it is composed with hydroxyl group, methylene bridge ( $CH_2-$ ) and ether bridge (C-O-C) connected between two aromatic rings, hence it is not discussed in this section.

Considering the infrared spectrum of n-C as shown in Figure 5.16 (a), it is clear that there are not any peaks at all spectrum regions. Hence, there are not any surface functional groups in the carbon monolith that prepared by carbonization with  $N_2$ .

According to Figure 5.16 (b), there are obvious peaks in four regions that consist with the broad band around 3434, 1625, 1114 and 811  $cm^{-1}$ . As mentioned before, peak assignment shown in Table 5.5, the peaks at 1625 and 811  $cm^{-1}$  can be attributed to stretching vibration of C=C and out-of-plane bending vibration of C-H, respectively, in the basal plane of the activated carbon. The broadly peak band around 1114  $cm^{-1}$  is difficult to assign because there is a superposition of a number of broad overlapping bands. However, they can be attributed to C-O-C stretching vibrations. Hence, these peaks may be attributed to the cyclic ether group on the surface of the activated carbon monolith. Moreover, the presence of peaks at 3434 and 1114  $cm^{-1}$  can also be assigned to the existence of the phenol group in the activated carbon.

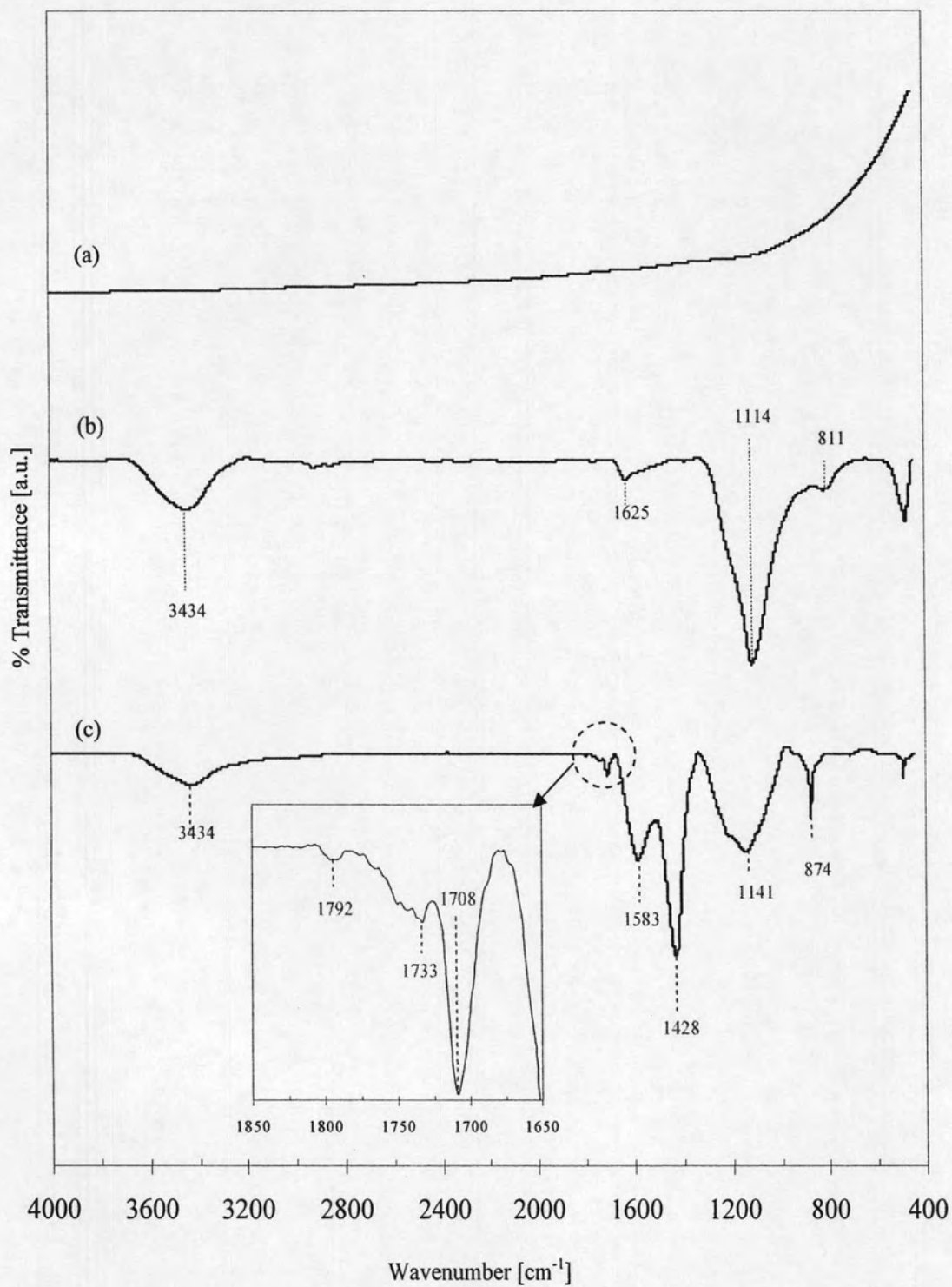


Figure 5.16: IR spectra of the carbon monoliths prepared by (a) N<sub>2</sub>-carbonization, n-C, (b) direct thermal activation c-C3 and (c) direct chemical activation, ca-C4.



According to Figure 5.16 (c), the peak bands around 3434, 1700, 1583, 1428, 1114 and 874  $\text{cm}^{-1}$  can obviously be observed. As previously mentioned peak assignment shown in Table 5.5, the peaks around 1583, 1428 and 874  $\text{cm}^{-1}$  are assigned to the stretching vibration mode of C=C, the bending vibration mode of C=C-H and the out-of-plane bending vibration of C-H, respectively, of the basal plane in the activated carbons. Moreover, the oxygenated functional groups (C=O and C-O) are reflected from the peak bands in the region of 1700 and 1114  $\text{cm}^{-1}$ , respectively. The peaks in the region of 1700  $\text{cm}^{-1}$  as shown in Figure 5.15 (c)-inset consist of 1792, 1733 and 1708  $\text{cm}^{-1}$ , whereas the peaks in the broad region of 1114  $\text{cm}^{-1}$  is difficult to assign because there is a superposition of a number of broad overlapping bands. However, they can be attributed either to C-O-C stretching vibrations in several forms or to C-OH stretching/bending mode. According to Table 5.5, it is possible to assign the oxygenated surface functional groups as followed;

- (1) The peaks at the broad range of  $\sim 3434$  and  $\sim 1114$   $\text{cm}^{-1}$  can be attributed to the phenol group (-OH stretching ( $\sim 3434$  and  $\sim 1000 - 1220$   $\text{cm}^{-1}$ ), O-H bending ( $\sim 1160 - 1200$   $\text{cm}^{-1}$ )).
- (2) The peaks at 1792, 1708 and 1114  $\text{cm}^{-1}$  can be attributed to the six-membered ring lactone group ( C=O stretching ( $\sim 1790$   $\text{cm}^{-1}$ ), C=O stretching induced by hydroxyl group ( $\sim 1710$   $\text{cm}^{-1}$ ) and C-O stretching ( $\sim 1160 - 1250$   $\text{cm}^{-1}$ )).
- (3) The peaks around 1733 and 1114  $\text{cm}^{-1}$  can be attributed to the five-membered ring lactone group (C=O stretching induced by hydroxyl group ( $\sim 1730$   $\text{cm}^{-1}$ ) and C-O stretching ( $\sim 1160-1250$   $\text{cm}^{-1}$ )).
- (4) The peak around 1114  $\text{cm}^{-1}$  can also be attributed to the cyclic ether group ( $\sim 1025 - 1141$   $\text{cm}^{-1}$ ).

In summary, the surface functional groups of the carbon monolith prepared by carbonization with  $N_2$  can not be observed. Meanwhile, the cyclic ether and the hydroxyl groups can be formed in the activated carbon monolith prepared by the direct thermal activation process. Furthermore, in the direct chemical activation process, the complex oxygenated functional groups consisting of the hydroxyl group and both six- and five-membered ring lactone groups can be obtained. It is clear that the termed "activated carbon monolith" is suitable for using with the carbon monolith derived from both the direct thermal activation and the direct chemical activation because of the existence of oxygenated functional groups. The oxygenated surface functional groups of these activated carbon monoliths as discussed above are shown in Figure 5.17.

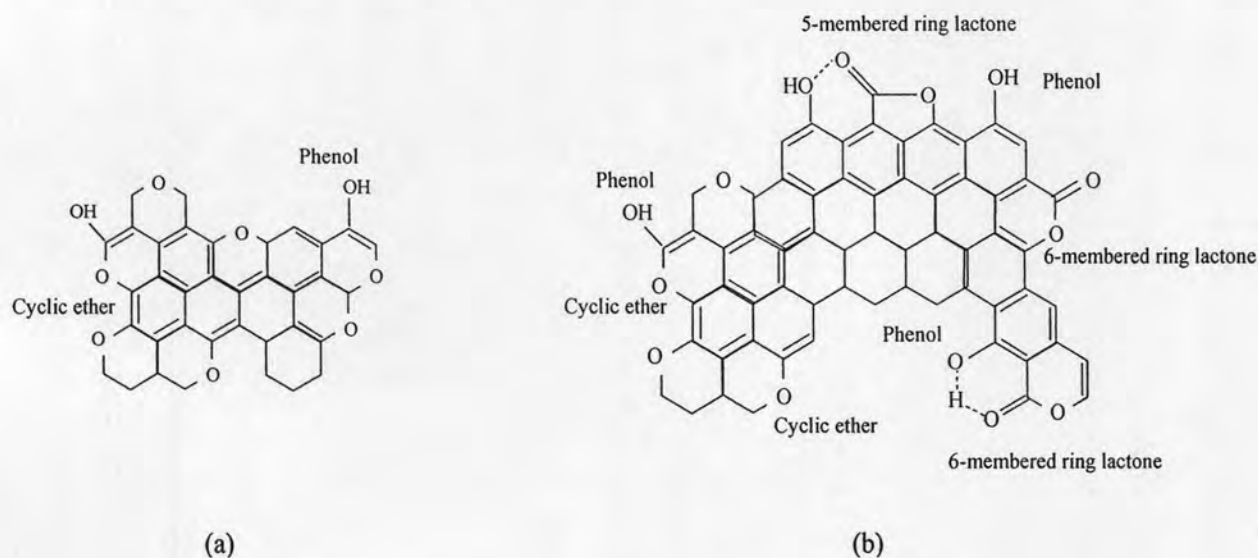


Figure 5.17: Schematic diagrams represented to the possibly oxygenated functional groups decorated at the edges of the polyaromatic of the activated carbon monoliths prepared by (a) direct thermal activation and (b) the direct chemical activation.

*The effect of activating temperature on the oxygenated functional groups of the activated carbon monoliths prepared by direct chemical activation*

The surface functional groups corresponding to the infrared spectrum of the RF monolith gel in Figure 5.18 (a) has been discussed in the section 4.2.1.3. They are

composed of methylene bridge ( $\text{CH}_2$ -) and ether bridge (C-O-C) connected between two aromatic rings.

After direct chemical activation process at the activating temperature of 500 °C, the infrared spectrum of the activated carbon monolith, ca-C1, is obtained as shown in Figure 5.18 (b). One can see that the peaks in the region of 1000 - 1300  $\text{cm}^{-1}$  corresponding with the stretching vibration of C-O bonding cannot merely be observed. There is a possibility that the functional groups of the ether bridge forms of the RF monolith gel are broken from processing condition. The peaks consisting of 3426, 1603, 1433, 1210 (shoulder) and 874  $\text{cm}^{-1}$  can be observed in the infrared spectrum as shown in Figure 5.18 (b). According to Table 5.5, the surface functional groups are proposed as followed:

- (1) The existence of the basal plane structure of the activated carbon can be referred by the peak at 1603 ( $\text{C}=\text{C}$  stretching vibration ( $\sim 1550\text{-}1650 \text{ cm}^{-1}$ )), the peak at 1433  $\text{cm}^{-1}$  (C-H bending vibration ( $\sim 1350\text{-}1550 \text{ cm}^{-1}$ )) and the peak at 874  $\text{cm}^{-1}$  (out-of-plane C-H bending vibration ( $\sim <900 \text{ cm}^{-1}$ )).
- (2) The low-concentration of phenol groups can be referred by the peak at 3426  $\text{cm}^{-1}$  (O-H stretching vibration ( $\sim 3400 \text{ cm}^{-1}$ )), the shoulder at 1210  $\text{cm}^{-1}$  (C-OH stretching ( $\sim 1000 - 1220 \text{ cm}^{-1}$ ) and O-H bending ( $\sim 1160 - 1200 \text{ cm}^{-1}$ )).

When the RF monolith gel is activated at the activating temperature of 800 °C, the infrared spectrum is obtained as shown in Figure 5.18 (c). One can see that the peaks in the regions of 1700 and 1200  $\text{cm}^{-1}$  corresponding to the existences of  $\text{C}=\text{O}$  and C-O, respectively, can be observed. It indicates that the complicate forms of the oxygenated surface functional groups can be obtained. According to the peaks in the region of  $\sim 1700 \text{ cm}^{-1}$  as shown in Figure 5.18 (c)-inset, they are located at the wavenumber of 1795, 1749 and 1707  $\text{cm}^{-1}$  that can be attributed to the presence of the six-membered ring lactone and the carboxylic groups according to Table 5.5. The broadly peak band around  $\sim 1200 \text{ cm}^{-1}$  is difficult to assign the surface functional groups because of superposition of many peaks. However, it may be assigned to the presence of cyclic ether groups ( $\sim 1025 - 1141 \text{ cm}^{-1}$ ). Meanwhile, the existences of the basal plane structure and the phenol groups are attributed with the peaks at 3433,

1582, 1430 and 874  $\text{cm}^{-1}$  as well as the activated carbon prepared at the activated temperature of 500 °C.

When the activating temperature reaches to 850 °C, the infrared spectrum is shown in Figure 5.18 (d). However, this spectrum has been discussed in above section already. They consist with the cyclic ether groups, six-membered ring lactone groups, five-membered ring lactone groups and phenol groups.

In summary, the direct activation process can introduce the oxygen into the carbon surface of the carbon monolith. At the activating temperature of 500 °C the introduced oxygen is mostly formed as the surface functional groups of the phenol groups decorated on the edge of the carbon basal plane. When the activation temperature increases the introduced oxygen is rearranged in various forms of the oxygenated functional groups. The oxygenated surface functional groups of the activated carbon monoliths prepared by the direct chemical activation at various activating temperatures are proposed in Figure 5.19.

### 5.3 Conclusions

An effective process in the preparation of carbon monolith with hierarchical porous structure is the focus in this chapter. The RF monolith gel with the interconnected macroporous structure prepared by sol-gel reaction assisted with ultrasonic irradiation is used as the carbon precursor. The carbonization, the direct thermal activation and the direct chemical activation are selected as micro-/mesoporosities generation processes. The carbonization process is carried out by heating the RF monolith gel under  $\text{N}_2$  gas flow. The direct thermal activation process is conducted by direct heating the RF monolith gel with  $\text{CO}_2$  gas, while the direct chemical activation process is carried out by impregnation of  $\text{Ca}(\text{NO}_3)_2$  into the RF monolith gel and followed by direct heating with  $\text{CO}_2$ . The results of this chapter can be concluded as followed.

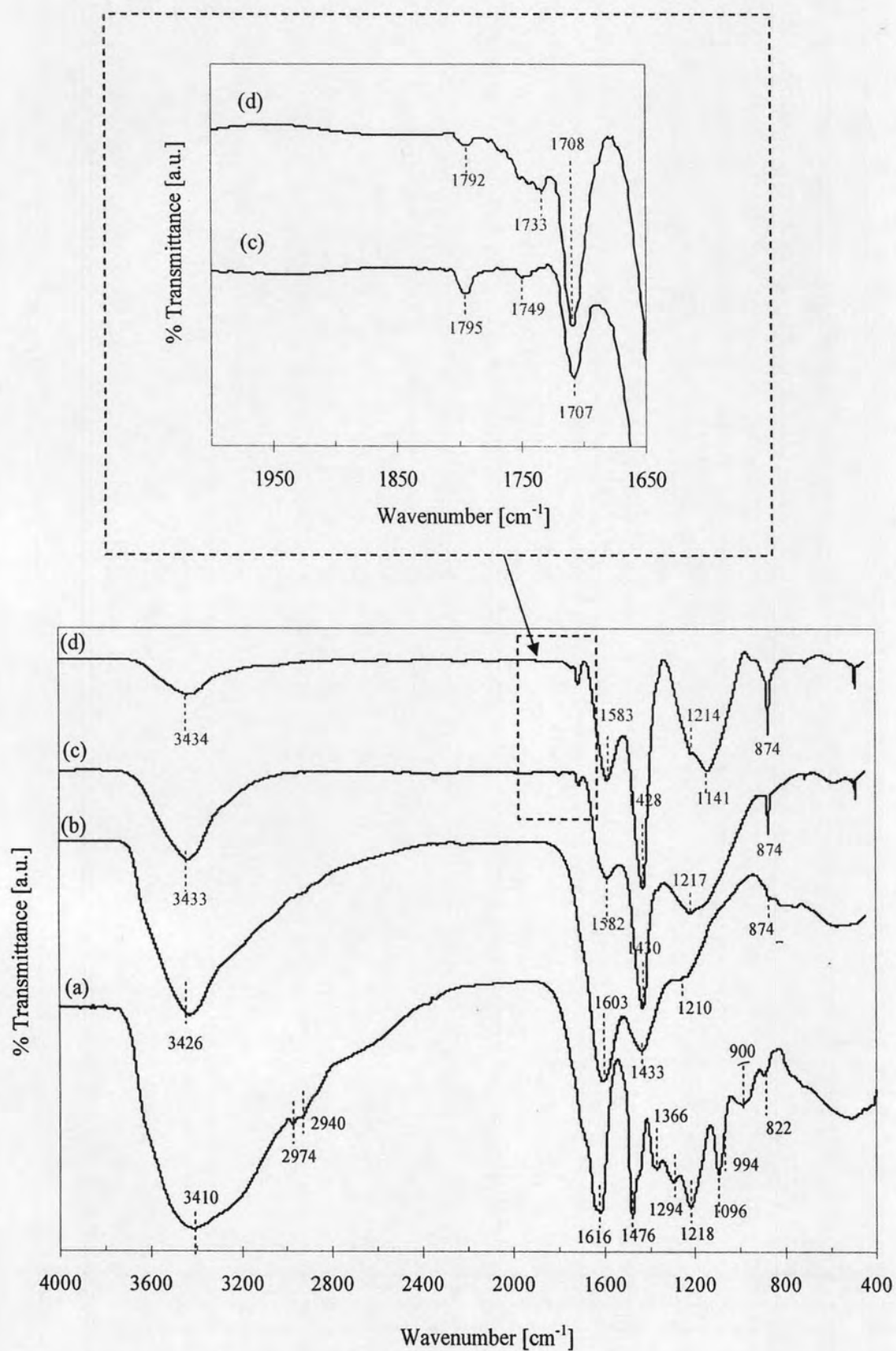


Figure 5.18: (a) IR spectra of (a) the RF monolith gel, and the carbon monoliths prepared by direct chemical activation at  $T_D$  of (b)-500 (ca-C1), (c) 800 (ca-C3) and (d) 850 °C (ca-C4).

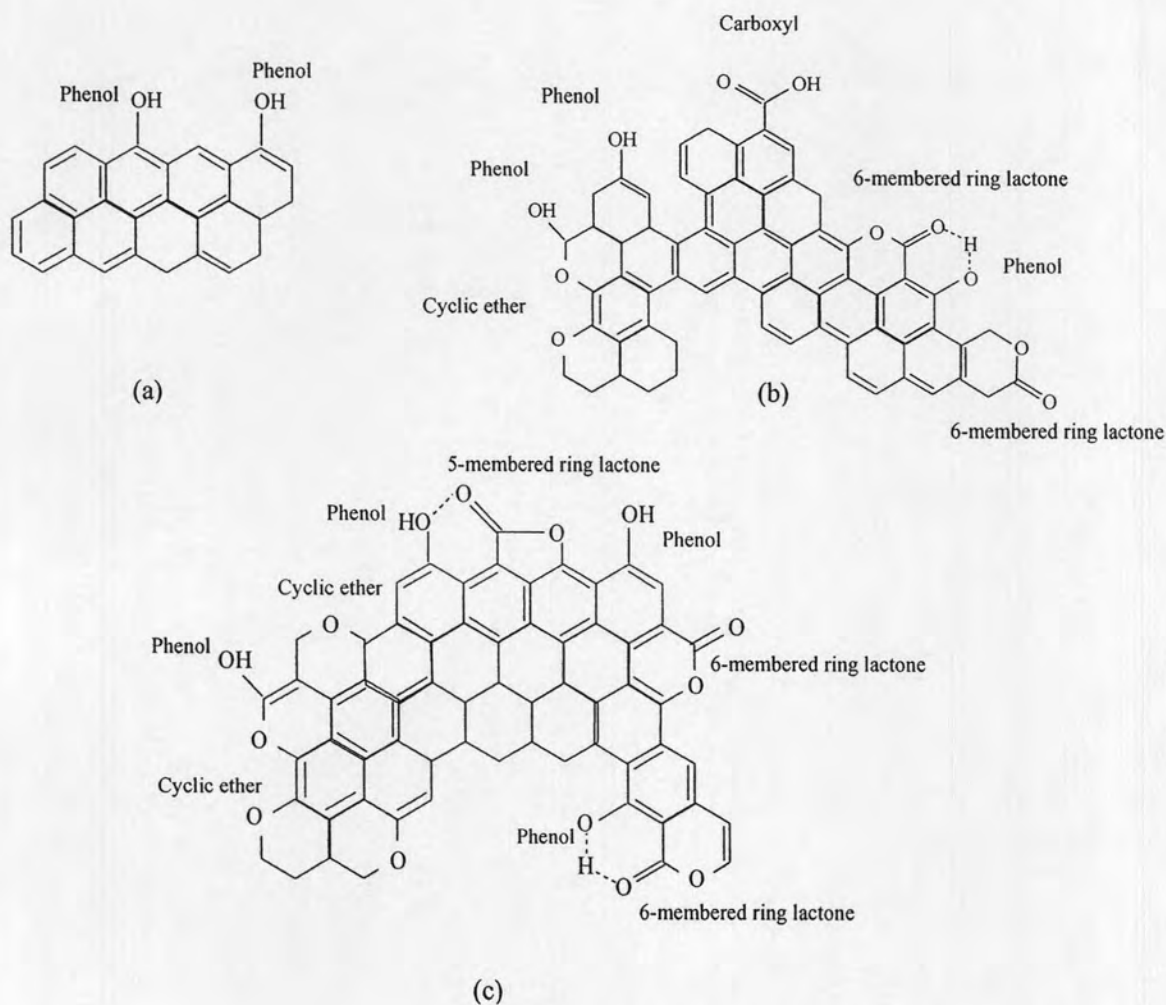


Figure 5.19: Possibilities of the oxygenated surface functional groups, interpreted from the infrared spectra of the activated carbon monoliths direct chemical activation at the activation temperature of (a) 500, (b) 800 and (c) 850 °C.

### Carbon monolith prepared by carbonization with $N_2$

1. The monolith form with the interconnected macroporous structure can be maintained after carbonization with  $N_2$ .
2. After carbonization, the microporosities are only generated on the interconnected macroporous structure. Therefore, the hierarchical bimodal micro-/macroporous carbon monolith can be prepared by this process.

3. From FT-IR result, there are not oxygenated surface functional groups in the carbon monolith prepared by carbonization process. In this case, the carbonization is carried out at 850 °C.

#### Carbon monolith prepared by direct thermal activation

1. Both monolith form and interconnected macroporous structure of the carbon monolith can be maintained after activation with CO<sub>2</sub> even when activating temperature reaches 900 °C.
2. Microporosities can only be generated on the interconnected macroporous structure of the obtained carbon monolith, therefore, the hierarchical bimodal micro-/macroporous carbon monolith can be prepared by this process.
3. Both micropore volume and specific surface area of the activated carbon monolith are improved with increasing the activating temperature.
4. The activated carbon monolith with high surface area (~900 m<sup>2</sup>/g) can be activated at 900 °C in a short retention time (30 min).
5. The oxygen elements on the surface of the activated carbon monolith are discovered in the form of surface functional groups of phenol and cyclic ether.

#### Carbon monolith prepared by direct chemical activation

1. At 30 min activation time, the activated carbon monolith with both monolithic shape and interconnected macroporous structure can be obtained when the activating temperature is lower than 900 °C.
2. At 850 °C activation temperature, the activated carbon monolith with both monolithic shape and interconnected macroporous structure can be obtained when the activating time is shorter than 120 min.
3. Not only microporosities but also mesoporosities can be generated on the interconnected macroporous structure. Therefore, the direct chemical activation can be used to prepare the activated carbon monolith with hierarchical tri-modal micro-/ meso-/macropores within the internal structure.

4. The activated carbon monolith both with hierarchical tri-modal micro-/meso-/macropores and high specific surface area ( $\sim 800 \text{ m}^2/\text{g}$ ) can be prepared in a single step and short retention time by the direct chemical activation.
5. At the short activating time ( $\sim 30 \text{ min}$ ), the activated carbon monolith with hierarchical tri-modal micro-/meso-/macropores can be achieved when the activating temperature is in the range of  $700 \text{ }^\circ\text{C}$  to  $900 \text{ }^\circ\text{C}$ . The mesoporosities cannot be obtained if the activating temperature is lower than  $700 \text{ }^\circ\text{C}$ , whereas the monolith cracks when the activating temperature reaches  $900 \text{ }^\circ\text{C}$ .
6. The suitable activating time at the activating temperature of  $850 \text{ }^\circ\text{C}$  for the preparation of the activated carbon monolith with hierarchical tri-modal micro-/meso-/macropores must be kept shorter than  $120 \text{ min}$  to avoid the cracking of monolith structure.
7. In direct chemical activation process, the complex oxygenated functional groups consisting of the hydroxyl group and both six- and five-membered ring lactone groups can be obtained when compared with the direct thermal activation process at the same  $T_D$   $850 \text{ }^\circ\text{C}$ .
8. At the activating temperature of  $500 \text{ }^\circ\text{C}$  the introduced oxygen is mostly formed as the surface functional groups of the phenol groups decorated on the edge of the carbon basal plane. When the activation temperature increases the introduced oxygen is rearranged in various forms of the oxygenated functional groups such as the hydroxyl, carboxylic, and both six- and five-membered ring lactone groups.